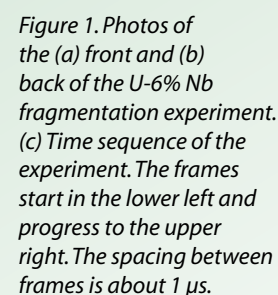


When energetic charged particles travel through matter, the Coulomb force between the particles and the atomic nuclei in the medium leads to a large number of small deflections of the particle trajectories. The nature of the Coulomb interaction leads to a cross section for scattering that is not integrable, but, in aggregate, the multiple scattering of a particle can be treated analytically.¹ To a good approximation, the angular distribution that results when a particle of momentum p traverses from a length of material l is given by

$$\frac{dN}{d\Omega} = \frac{1}{2\pi\theta_0^2} e^{-\frac{\theta^2}{2\theta_0^2}}, \quad (1)$$
$$\theta_0 = \frac{14.1}{p\beta} \sqrt{\frac{l}{X_0}}. \quad (2)$$
$$X_0 = \frac{716}{Z(Z+1)\ln(287/\sqrt{Z})}. \quad (3)$$

Charged particles also scatter from electrons in the medium. Because the electrons are light, charged-particle scattering generally leads to continuous energy loss rather than to angular deflections. This energy-loss mechanism provides a method for detecting the particles. In proton and electron radiography, images can be formed on scintillator screens with high efficiency. For cosmic-ray muon radiography, the energy deposited in a multiwire drift detector is used to measure the trajectory of individual cosmic rays. Multiple scattering leads to a stochastic trajectory through the medium. This is one of the limitations of charged-particle radiography. Position resolution is ultimately limited by the scale established by the product, multiple-scattering angle, and object thickness, $\Delta x = k\theta_0 l$, where k is a charge dependent constant of order unity.



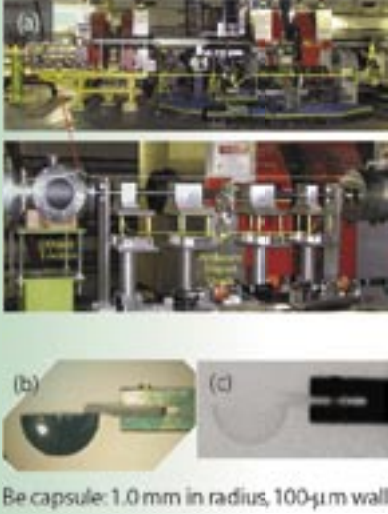


Figure 2. Photo of (a) the newly commissioned magnifier with images of one-half of a beryllium capsule (b) and its radiograph (c).

Radiography 2003

Proton radiography. Charged particles are bent by the Lorenz force in a magnetic field. Lenses that focus charged particle beams can be constructed from quadrupole magnets. Highly symmetric lens systems have been developed for pRad that sort the scattering angles in a beam transmitted by an object in one plane (the Fourier plane); these lenses then form an image of the transmitted beam in another plane (the image plane) further downstream.

Proton radiography was originally developed to take advantage of the enormous gain in statistical precision that can be obtained by using the long, hadronic mean-free path of protons, $\lambda_p = 200 \text{ gm/cm}^3$, when compared to the relatively short mean-free path of high-energy photons, $\lambda_\gamma = 25 \text{ gm/cm}^3$, for thick-object hydrotest radiography. This has been studied at the AGS at BNL using higher-energy proton beams (24 GeV/c) than those available at LANL (1.4 GeV/c), and indeed the expected advantage of about a factor of 100 over the first axis of DARHT has been demonstrated.²

The 800-MeV proton beam provided by the LANSCE accelerator has proven to be very useful for smaller-scale experiments, even though this energy is too low for hydrotest radiography, by using the principles laid out above. A collimator placed in the Fourier plane controls the contrast in the image plane by adjusting its size to provide the optimum contrast for a given experiment. The transmission through an object using a collimator that passes the transmitted beam up to some maximum angle, θ_c , can be calculated by integrating Equation 1:

$$t_{\text{tr}} = \int_0^{\theta_c} \frac{1}{\theta_0^2} e^{-\frac{\theta^2}{2\theta_0^2}} \sin(\theta) d\theta, \quad (4)$$

which for small angles gives

$$t_{\text{tr}} = (1 - e^{-\frac{\kappa}{l}}), \quad (5)$$

where

$$\kappa = \frac{\theta^2 p^2 \beta^2 X_0}{14 l^2} \quad (6)$$

Here, κ is the thickness scale set at the collimator angle cut. The collimator angle can be chosen to optimize the measurement of l for the most interesting part of an experiment for a given

incident number of particles, N_0 :

$$\frac{\Delta l}{l} = \frac{l}{\kappa} \frac{\sqrt{t_{\text{tr}}}}{1 - t_{\text{tr}}} \frac{1}{\sqrt{N_0}} \quad (7)$$

Equation 7 can be solved for a minimum as a function of κ . The result is $\kappa = 0.64 l$ (i.e., a transmission of 47%). From the discussion above, one sees that within the limits imposed by beam luminosity, pRad can be used for dynamic radiography on thin and thick systems. This is the observation that has made the pRad facility at LANSCE so useful to the weapons program.

Deuterium-uranium experiment. The fragmentation of shocked pieces of metal has been experimentally studied since the Civil War³ to obtain information needed for designing ordnance. Recently, models have been developed and incorporated into computer codes that may for the first time allow this phenomenon to be predicted.⁴ X-ray radiography can provide detailed snapshots of fragments in material at high strain rates in explosively driven experiments. The single images obtained cannot follow the time development of the material damage, and they are not quantitative. Although the x-ray experiments have been of great importance in the model development, pRad has been pursued because it can follow the time development of a single experiment (which is important because of the stochastic nature of these phenomena) and because it can provide quantitative data.

A recent series of experiments were performed on a strategically interesting material—uranium alloyed with 6% niobium. Small shells of this material were put under biaxial strain using a point-detonated hemispherical charge. A photo of one of these experiments along with a series of pRad images is shown in Figure 1. As can be seen, the fragmentation of the metal can be clearly followed.

Magnifier. Much the same as with an optical microscope, charged-particle images can be magnified using magnetic lenses. We have recently commissioned a proton magnifier (Figure 2) that uses permanent magnets to provide an enlarged image. Magnification also reduces the contribution of aberrations to the position resolution of the final image. As a consequence, the magnifier produced images with position resolution that is better than $15 \mu\text{m}$ over a 2-cm field of view, which is much better than the $200 \mu\text{m}$ that we have obtained with our larger lenses. This smaller field of view can be illuminated to a relatively high particle density with very short pulses from the LANSCE proton beam. We hope to perform studies of explosives and explosively driven phenomena on a much shorter length scale using this magnifier.

Charged-Particle Radiography—Providing New Methods of Imaging

Electron radiography. The NIF being built at LLNL has a goal of reaching thermonuclear ignition by driving the spherical implosion of a DT ice layer frozen to the inside of a capsule that is imploded using x-rays generated by very high-power laser beams. The time scale of the implosion is about 20 ns. The spatial and time scales and the dynamic range provide a challenge for existing diagnostics. The required position resolution of better than 10 μm can be obtained with charged-particle radiography using a magnifier. However, it would be difficult, as well as expensive, to obtain enough luminosity with a proton beam for this task.

We have performed studies of electron radiography to determine if it can cover the dynamic range of a NIF implosion. Because electron sources are very bright, we have shown that the intensity needed can be obtained from existing sources. Simulated radiographs at $t = 0$ and at $t = 17$ ns, nuclear time, for a NIF capsule are shown in Figure 3 for a simple permanent-magnet magnifier and a 400-MeV electron beam. These results indicate that the electrons may provide a unique diagnostic. Further theoretical studies are needed to ensure that the coupling between the electrons and the plasma do not perturb the image. Meanwhile, an electron accelerator and lens are being built at LANL to further study the experimental issues in electron radiography. The goal of this work is to provide a diagnostic tool for static radiography aimed at studying the uniformity of the ice layer inside of NIF capsules.

Muon radiography. An explosion, or even a fizzle, of a nuclear device in a major city would be catastrophic. The likelihood of such an attack from terrorist activities has been placed at 0.1–0.01 per year.⁵ The direct consequences in deaths and economic damage would dwarf the destruction of the World Trade Centers. The aftermath would be likely to shut down international trade. The impact on world economies would be enormous. Strategies to prevent nuclear weapons or the components needed to build them from becoming available to terrorists are currently being formulated. Components include tightly controlling the world's supply of fissile materials, reducing or diluting the material that is suitable for building nuclear weapons, and providing surveillance at transportation choke points to interdict the illicit transport of fissionable materials.

The essential component of any nuclear explosive device is the fissile core. This material is radioactive, emitting gamma rays, alpha particles, and neutrons. Both gamma radiation and neutron emission allow detection at a distance of meters. Detection schemes deployed to date have measured the gamma radiation or have used horizontal x-ray radiography

to try to image the material. The gamma radiation, however, is easily shielded with a few centimeters of lead, tungsten, or other heavy metal, and the radiography has been shown to be ineffective. X-ray radiography with currently deployed test systems has failed to detect shipments of depleted uranium.

We have investigated the feasibility of using cosmic-ray muon radiography for homeland defense and compared the process to other active radiography approaches. In muon radiography, the charged particles are cosmic-ray muons. Because of their low rates, the muons can be individually detected.

Conventional radiography takes advantage of the absorption of penetrating radiation. For x-ray radiography,⁶ the brightness of a pixel in the image is determined by the absorption or scattering of the incident beam:

$$N = N_0 e^{-\frac{L}{L_0}}, \quad (8)$$

where L is the path length (areal density) through an object, and L_0 is the mean-free path for scattering or absorption. The precision of radiographic measurements is limited by Poisson counting statistics of the transmitted flux,

$$\frac{\Delta L}{L_0} = \frac{1}{\sqrt{N}}. \quad (9)$$

The maximum mean-free path for photons in high-Z elements occurs at a few MeV. The mean-free path is approximately 25 gm/cm^2 for all materials at this energy. This corresponds to less than 2 cm of lead. To penetrate objects of tens of L_0 requires a large incident dose. An alternative is provided by charged-particle² radiography using cosmic-ray muons. In a 10-cm-thick layer, a 3-GeV muon (the average cosmic-ray energy) will scatter with a mean angle of 2.3 mrad in water ($X = 36$ cm), 11 mrad in iron ($X = 1.76$ cm), and 20 mrad in tungsten ($X = 0.56$ cm). If the muon-scattering angle in an object can be measured and if its momentum is known, then the path length, L , can be determined to a precision of

$$\frac{\Delta L}{L} = \sqrt{\frac{2}{N}}, \quad (10)$$

where N , the number of transmitted muons, is very nearly equal to the number of incident muons. Thus, each transmitted muon provides information about the thickness of the object.

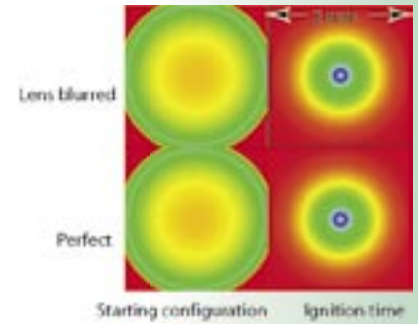


Figure 3. Simulated radiographs at $t = 0$ and $t = 17$ ns for a NIF capsule.

Facilities Research Highlights

We have constructed models of realistic shipping containers and vehicles for use in the Monte Carlo radiation codes known as MCNPX⁷ and GEANT.⁸ These have been used to compare existing x-ray and gamma-ray techniques with muon radiography. Muon radiography has been shown to discriminate all of the scenarios considered in less than four minutes scanning time. In Figure 4, a container has been filled with two layers of half-density iron balls, 20 cm in radius on 50-cm centers. A 20-kg sphere of high-enriched uranium has been hidden in the container. The muon radiograph in Figure 4 clearly shows the ease with which nuclear materials can be distinguished from background scatter. An x-ray radiography of a portion of the container, also shown in Figure 4, is plagued with problems from background scatter. Also, x-ray radiography does not provide three-dimensional views of a scene. Two-view x-ray radiography may be able to address some of these problems. The results of this study show that within the boundaries of weight limits, shielded containers of fissionable material can be easily obscured in ways that make it impossible to discriminate the material from legitimate cargo with x-rays. However, these are easily detected using muon radiography.

Conclusion

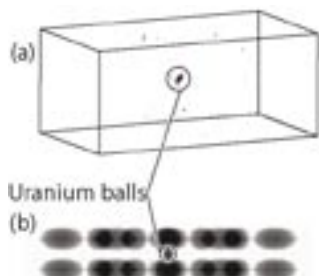
Charged-particle radiography is providing a versatile new probe that has advantages over conventional x-ray radiography for some unique applications. In pRad, charged-particle radiography has been used to make quantitative motion pictures of dynamic events. By taking advantage of magnetic lenses to magnify images and by using the very bright beams that can be made with electrons, we

have suggested that charged-particle radiography might even be useful for studying the fine spatial detail and very fast motion in a NIF implosion. Finally, we have demonstrated that radiographs can be made using cosmic-ray muons for homeland-defense applications.

References

1. B. Rossi, *High-Energy Particles* (Prentice-Hall, NJ, 1952), p. 66.
2. C.L. Morris *et al.*, "A comparison of proton and x-ray thick object radiography," *Defense Review*, to be published (2003).
3. G.T. Gray, private communication, 2003.
4. P.J. Maudlin, Weapons Working Group, Los Alamos National Laboratory, December 2003.
5. S.E. Koonin, "Concealed nuclear devices," Jason Fall Meeting, McClean, Virginia, 2003.
6. N.B. Konstantin, G.E. Hogan, C. Morris, W.C. Priedhorsky, A. Saunders, L.J. Schultz, and M.E. Teasdale, "Radiographic imaging with cosmic ray muons," *Nature* **422**, 277 (2003); W.C. Priedhorsky *et al.*, "Detection of high-Z objects using multiple scattering of cosmic ray muons," *Review of Scientific Instruments* **74**, 4294-4297 (2003); and L.J. Schultz, K.N. Borozdin, J.J. Gomez, G.E. Hogan, J.A. McGill, C. Morris, W.C. Priedhorsky, A. Saunders, and M.E. Teasdale, "Image reconstruction and material Z discrimination via cosmic ray muon radiography," *Nuclear Instruments and Methods in Physics Research*, in press (2003).
7. J.S. Hendricks *et al.*, "MCNPX, Version 2.5.c," Los Alamos National Laboratory report LA-UR-03-2202, (2002).
8. Application Software Group Computing and Networks Division, "GEANT detector description and simulation tool," CERN Program Library (W5013), <http://wwwasdoc.web.cern.ch/wwwasdoc/pdfdir/geant.pdf>.

Figure 4. (a) Muon-radiography result. The uranium is visible and easily detectable above a threshold automatically. (b) X-ray result. The contrast has been reduced by scatter background. The uranium is not easily detectable automatically and cannot be distinguished from the iron cargo automatically. It could be moved so that it is shielded by the iron.



For more information, contact Chris Morris at 505-667-5652, cmorris@lanl.gov.